Implications of the Optical Observations of Isolated Neutron Stars

Andy Shearer, Aaron Golden

andy.shearer@nuigalway.ie, aaron.golden@nuigalway.ie

The National University of Ireland, Galway, Newcastle Road, Galway, Ireland

Received ______________; accepted ______________

To appear in ApJ

ABSTRACT

We show that observations of pulsars with pulsed optical emission indicate that the peak flux scales according to the magnetic field strength at the light cylinder. The derived relationships indicate that the emission mechanism is common across all of the observed pulsars with periods ranging from 33ms to 385 ms and ages of 1000-300,000 years. It is noted that similar trends exist for γ ray pulsars. Furthermore the model proposed by Pacini (1971) and developed by Pacini and Salvati (1983,1987) still has validity and gives an adequate explanation of the optical phenomena.

1. Introduction

Since the first optical observations of the Crab pulsar in the late 1960s ((4)), 7 more pulsars have been observed in the optical bandpass. Of these only 4 have been seen to pulsate optically (PSR0540-69, (20); Vela, (37); PSR 0656+14, (32); Geminga, (33)). Whilst the three remaining pulsars (PSR0950+08, PSR 1929+10 and PSR1055-52) are thought to be mainly thermal emitters in the optical regime, the pulsating objects are either purely magnetospheric emitters or a mixture of thermal and non-thermal sources. Two of these five pulsars (PSR0540-69 and the Crab) are certainly too distant to have any detectable optical thermal emission using currently available technologies. For those with distances less than a kiloparsec (Geminga, Vela and PSR0656+14) only the Vela pulsar is too bright for its emission to be anything other than non-thermal in origin. For the remaining two pulsars (PSR0656+14 and Geminga) their optical emission is thought to be a mix of thermal and non-thermal fluxes ((8) and (18)). However for the faintest of the two, Geminga, there is disagreement about the level of thermal emission. Broad-band photometric studies have been interpreted as being consistent with the Rayleigh-Jeans tail combined with a cyclotron emission feature ((21)). These authors suggest that the optical emission is predominantly thermal with an embedded ion cyclotron resonance feature at about 5500 Å. More recently, (14), derive a complex phenomenological model for this feature coming from a thin plasma above the pulsar's polar cap. Their derived surface magnetic field using this model is consistent with the independently determined 'spin-down' field ($B \propto (P\dot{P})^{0.5}$). Conversely, spectroscopic studies have indicated that the emission is a mix of thermal and non-thermal radiation with the non-thermal dominating in the optical region ((18)). These authors do not see the proposed emission feature, but, there is a statistically weak absorption feature at 6400Å. Temporal studies of the pulsars indicate that for the Crab and Vela pulsars the peak of γ-ray and optical pulses are coincident. A similar coincidence is noted for the Geminga pulsar although the optical signal is of lower significance. This can interpreted as indicating a common source location for both γ and optical photons. Recent studies of the plateau of the Crab main pulse in the optical indicate that it is of limited (< 15 kms) extent ((9)).

Many suggestions have been made concerning the non-thermal optical emission process for these young and middle-aged pulsars. Despite many years of detailed theoretical studies and more recently limited numerical simulations, no convincing models have been derived which explain all of the high energy properties. There are similar problems in the radio but as the emission mechanism is radically different (being coherent) only the high energy emission will be considered here.

In recent years a number of groups have carried out detailed simulations of the various high-energy emission processes. These models divide into two broad groups - those with acceleration and emission low in the magnetosphere (polar cap models) and those with the acceleration nearer to the light cylinder (outer-gap models). Both models have problems explaining the observed features of the limited selection of high energy emitters. Both models also suffer from arbitrary assumptions in terms of the sustainability of the outer-gap and the orientation of the pulsar's magnetic field to both the observers line of sight and the rotation axis. Furthermore some observational evidence, see for example (6), severely limits the applicability of the outer-gap to the emission from the Crab pulsar. However these models have their successes - the total polar-cap emission can be understood in terms of the Goldreich-Julian current ((12)) from in or around the cap; the Crab polarisation sweep is accurately reproduced by an outer-gap variant of (30). However, the most successful model which adequately explains most of the high-energy phenomena (both in terms of its elegance and longevity) has been proposed by (26) and in modified form by Pacini and Salvati (1983 PS83 & 1987 PS87 hereafter). In general they proposed that the high energy emission comes from relativistic electrons radiating via synchrotron processes in the outer regions of the magnetosphere and that the luminosity is a strong function of the period ($\propto P^{-10}$ in the original formulation). In this paper we examine the validity of their approach and show that it still adequately explains the observed phenomena.

It is the failure of the detailed models to explain the high energy emission that has prompted this work. We have taken a phenomenological approach to test whether Pacini type scaling is still applicable. Our approach has been to try to restrict the effects of geometry by taking the peak luminosity as a scaling parameter rather than the total luminosity. In this regard we are removing the duty cycle term from PS87. It is our opinion that to first order the peak emission represents the local power density along the observer's line of site and hence reflects more accurately emission processes within a pulsar's magnetosphere. Previous work in this area (see for example (11)) looked at the total efficiency, spectral index and found no reasonable correlation with standard pulsar parameters - age, period and spin down rate. Their work was hampered by not including geometry and being restricted to the then three known pulsed optical emitters. Since then the number of pulsars with observed pulsed optical emission has increased to five.

2. The Phenomenology of Magnetospheric Emission

The three optically brightest pulsars (Crab, Vela and PSR 0540-69) are also amongst the youngest. However all these pulsars have very different pulse shapes resulting in a very different ratio between the integrated flux and the peak flux. In this work we will use the peak emission as the primary flux parameter. A number of definitions can exist for this and in this context we have taken the 95%-95% level of the primary pulse. To first order, this correlates well with the luminosity per pulse divided by the Full-Width at Half-Maximum (FWHM). For the Crab pulsar the cusp is effectively flat over this region ((10)). The FWHM can be considered to scale with the pulsar duty cycle. Our proposition is that the peak flux represents the local power density within the emitting region with minimal effects from geometrical considerations such as observer line of sight and magnetic and rotational axis orientation. Table 1 shows the basic parameters for these objects including the peak emission (taken as the emission in the 95% - 95% portion of the largest peak). Their distances imply that the thermal emission should be low, in all cases $< 1\%$ of the observed emission, and any such contribution is negligible.

Of all the optical pulsars Geminga is perhaps the most controversial. Early observations ((16), and (2)) indicated that Geminga was an ≈ 25.5 m_V object. Subsequent observations including HST photometry appeared to support a thermal origin for the optical photons, albeit requiring a cyclotron resonance feature in the optical ((21)). The high-speed optical observations of (33) combined with spectroscopic observations ((18)) contrast with this view. Figures 1 and 2 show how this apparent contradiction could have arisen. Figure 1, based upon data from (21) shows the integrated photometry. It is possible to fit a black body Rayleigh-Jeans tail through this, but only with the fitting of a cyclotron resonance emission feature at about 5500 Å. Figure 2 however shows the same points plotted on top of the Martin et al spectra, where we have also included the pulsed B point ((33)). All the data points are consistent within their error bars. This combined data set indicates a fairly steep spectrum (with spectral index of 1.9) consistent with magnetospheric emission and a weak thermal component, without the requirement for a cyclotron feature. It was on the basis of these results that (8) were able to give an upper limit of R_∞ of about 10km, by considering the upper limits to the unpulsed fraction of the optical emission from Geminga as an upper limit for the thermal emission. A simpler view is that the soft X-ray and EUV data is predominantly thermal emission with a magnetospheric component becoming dominant at about 3500 Å. Figure 3 illustrates this with the thermal and magnetospheric components from (8) combined with the broad-band points of (21) and (33). We should also note that the optical pulses seen by (33) are coincident with the observed γ ray peaks. Clearly more spectroscopic data, particularly if temporally resolved, will be crucial to determining the exact mix of thermal and non-thermal emission.

As regards PSR 0656+14 the pulsar is generally agreed to be predominately a non-thermal emitter in the optical, becoming predominantly a thermal emitter at wavelengths shorter than about 3000Å((25)). However, there is a discrepancy between the radio distance based upon the dispersion measure and the best fits to the X-ray data. From radio dispersion measure a distance of $760 \pm 190pc$ can be derived, at odds with the X-ray distance of $250 - 280pc$ from N_H galactic models. Clearly more observations are needed to determine a parallax - both radio and optical. This discrepancy in distance leads to an ambiguity in the total luminosity. For this paper we have taken the lower distance measure.

In Table 1 we have indicated the peak flux normalised to the Crab pulsar. When comparing the individual pulsars, which will have a range of viewing angles and differing magnetic/rotation axes, we have to account for the viewing angle (related to the pulse duty cycle and separation) as well as the total flux. Furthermore for each source, we have to account for the shape of the pulsar's spectrum. For all the observed pulsars, with the exception of Vela, the low energy cut-off is above 7000 Å((23)). PS87 indicates for emission above the low energy cut-off that the ratio of the fluxes from two different pulsars can be given by Equation 1 if one ignores the effect of duty cycle and pitch angle (the suffices refer to each pulsar). Here $F_{\nu,n}$ refers to the flux at the observed frequency ν for pulsar n. Similarly for the magnetic field strength, B, and period, P. The observed energy spectrum exponent is given by α_n. The duty cycle can be accounted for by only considering the peak emission. The pitch angle is beyond the scope of this work and assumed to first order to be invariant. Equation 2 shows the the same formulation for the outer field case.

$$\frac{F_{\nu,2}}{F_{\nu,1}} \propto (\frac{\nu_{1,0}}{\nu})^{\alpha_2-\alpha_1}(\frac{B_{2,0}}{B_{1,0}})^{4-\alpha_2}(\frac{P_2}{P_1})^{3\alpha-9} \tag{1}$$

Scaling to the transverse field would give:-

$$\frac{F_{\nu,2}}{F_{\nu,1}} \propto (\frac{\nu_{1,0}}{\nu})^{\alpha_2-\alpha_1}(\frac{B_{2,0}}{B_{1,0}})^{4-\alpha_2}(\frac{P_2}{P_1})^{3} \tag{2}$$

Given the observed peak luminosities we investigated the correlation between the peak emission and the surface field and the tangential light cylinder field. Figure 4 shows the relationship between the peak luminosity and the outer magnetic field, B_T, Goldreich-Julian current and canonical age ($\frac{P}{2\dot{P}}$). A clear correlation is seen with all these parameters. In this paper we investigate the implications of a correlation between the peak luminosity and the transverse field. We accept that the strong correlation with G-J current would underpin both emission from polar cap as well as outer regions.

A weighted regression of the form :-

Peak Luminosity $\propto B_T^{\beta}$

was performed for the empirical peak luminosity leading to a relationship of the form :-

Peak Luminosity $\propto B_T^{2.86 \pm 0.12}$

which is significant at the 99.5% level. Figure 5 shows the predicted peak luminosity from Equation 2 against our observed peak luminosity accounting for the differing observed energy spectrum exponent at 4500 Å. The slope is 0.95 ± 0.04 and significant at the 99 % level. Importantly, we note that the flattening of the peak luminosity relationship with the outer field strength for the older, slower pulsars, see Figure 4, is consistent with their having a significantly steeper energy spectrum than the younger pulsars, see Table 1. Whilst, from PS87, it is possible that this indicates that the emission zone is optically thick at these frequencies, alternatively it might reflect a larger emission region for these pulsars compared to the younger ones. We also note that the generation parameter concept ((38)) indicates that the γ-ray spectral index scales with the average number of generations within the e^+/e^- cascade. Our observed correlation between peak luminosity and age (which linearly scales with the generation parameter) and similarly between spectral index and age indicates a link between optical luminosity and γ-ray luminosity phenomena.

We note as well as that similar trends can be seen in γ-rays. Figure 6 shows the correlation between the peak γ emission as a function of transverse field. This indicates a regression of the form

Peak γ Luminosity $\propto B_T^{0.86 \pm 0.17}$

significant at the 99.3 % level, consistent with the observed steeper distribution seen in high energy γ-rays - see Table 2 and Equation 2.

It seems clear from both polarisation studies ((34); (30)) and from this work that we expect that the optical emission zone is sited towards the outer magnetosphere. Timing studies of the size of the Crab pulse plateau indicates a restricted emission volume (≈ 15 kms in lateral extent) ((9)). Importantly, the simple relationships we have derived here indicate that there is no need to invoke complex models for this high energy emission. Observed variations in spectral index, pulse shape and polarisation can be understood in terms of geometrical and absorption factors rather than differences in the production mechanism.

Combining our results and those of (11), we can begin to understand how the high energy emission process ages. Goldoni et al compared the known spectral indices and efficiencies in both the optical and γ-ray regions. They noted that the spectral index flattened with age for the γ-ray pulsars whilst the reverse was true for the optically emitting systems. They also noted a similar trend reversal for the efficiency, with the γ-ray pulsars becoming more efficient with age. We note (see the bottom panel in Figures 4 and 6) a similar behaviour with the peak emission. From the temporal coincidence between the γ-ray and optical pulses, it seems likely that the source location is similar for both mechanisms. One explanation is that we have a position where by from the same electron population there are two emission processes - expected if we have curvature for the γ-ray photons and synchrotron for the optical ones. It seems likely that the optical photon spectrum has been further modified to produce the reversal in spectral index with age. The region over which the scattering can occur would scale with the size of the magnetosphere and hence with age. With the outer magnetosphere fields for these pulsars being $< 10^6$ G, electron cyclotron scattering is not an option. However synchrotron self-absorbtion could explain the observed features. In essence we would expect the most marked flattening to be for the Crab pulsar, where the outer field strengths are of order 10^6 G, and less so for the slower and older systems.

These results (both optical and γ-rays) are consistent with a model where the γ and optical emission is coming from the last open-field line at some constant fraction of the light cylinder. The drop in efficiency with age for the production of optical photons points towards an absorbing process in the outer magnetosphere. Clearly more optical and γ-ray observations are needed to confirm these trends.

3. Conclusion

We have shown that the peak optical luminosity is the key important parameter that scales with other observed pulsar attributes. We note that similar behaviour can be seen in the γ-ray regime. To first order we confirm that the model first proposed by Pacini in 1971 still has validity. There is a proviso that there is a strong correlation with the Goldreich-Julian current which underpins both Pacini scaling and other models. From a more detailed anaysis of the EGRET database (19) showed a similar functional form to our derived relationship for the total luminosity against period and surface magnetic field. We also show in Table 3 what the expected luminosity would be from a number of X and γ-ray emitting pulsars. We have chosen these on the basis of their known duty cycles in the high energy regime. We have also considered the expected flux from the anomalous X-ray pulsars, a class of magnetars. If the observed P and $\dot{P}$ relationship can be interpreted in same way as for normal pulsars to derive a canonical surface field then we can estimate what the expected luminosity of these object would be. The derived luminosity is very low - a reflection of the weak light cylinder field. A recent VLT observation ((15)) has found no optical candidates down to 25.5 R magnitude - consistent with no magnetospheric emission and predominantly thermal output. Problems remain however as to the source of the thermal emission. We note that, in the outer magnetosphere of these objects, the magnetic field is far too weak for optical non-thermal emission processes.

Of crucial importance in the future will be the determination of the low-energy cutoff and the polarisation sweep through the optical pulse. Also of interest will be the shape of the pulse - in particular the size of any plateau which scales as the size of the emission zone. Optical observations of millisecond pulsars will also be important, to see if they follow the age or field trends noted here. Of interest in this regard is the result from X-ray observations which indicate that the luminosity of millisecond pulsars scales in a similar fashion to normal pulsars ((1)). All of these parameters are measurable with existing and emerging technologies and telescopes.

Finally, the recent detection of a 16 ms pulsar in the LMC (PSR J0537-6910 ((17)) which has defied optical detection despite its low period can possibly be understood in terms of its age ($\approx$ 5,000 years), which on the basis of Figure 3 indicates peak luminosity a factor of $\approx 10^5$ times lower than the Crab. This is at the limit of some of the recent optical searches - (22) and (13).

This work was supported by the Enterprise Ireland Basic Grant scheme whose assistance is gratefully acknowledged. Ray Butler is thanked for his helped during the preparation of the manuscript. He and Padraig O'Connor are thanked for useful comments during the course of this work. The anonymous referee is thanked for comments which improved an early draft of this paper.

REFERENCES

Becker, W. & Trümper, J., 1997, A&A, 326, 682

Bignami, G. F., Caraveo, P. A. & Paul, J. A., 1988, A&A, 202, L1

Bignami, G. F., Caraveo, P. A., Mignani, R., Edelstein, J. & Bowyer, S, 1996, ApJ, 456, L111

Cocke, W. J., Disney, M. J. & Taylor, D. J., 1969, Nature, 221, 525

Caraveo, P. A., Bignami, G. F., Mignani, R. & Taff, L. G., 1996, A&AS, 120, 65

Eikenberry, S. S. & Fazio, G. G., 1997, ApJ, 476, 281

Fierro, J. M., Michelson, P. F., Nolan, D. C. & Thompson, D. J., 1998, ApJ, 494, 734

Golden, A. & Shearer, A., 1999, A&A, 342, L5

Golden, A., Shearer, A., 2000, ApJ, 999, 99

Golden, A., Shearer, A. &Redfern, M, 2000, submitted to A&A

Goldoni, P., Musso, C., Caraveo, P. A. & Bignami, G. F., 1995, A&A, 298, 535

Goldreich, P. & Julian, W., 1969, ApJ, 245, 267

Gouiffes, C. & Ögelman, H, 2000, Pulsar Astronomy - 2000 and Beyond, ASP Conference Series, Vol. 202; Proceedings of the 177th IAU Colloquium 177 (San Francisco: ASP). Edited by M. Kramer, N. Wex, and N. Wielebinski, p. 301

Jacchia, A., de Luca, F., Lazzaro, E., Caraveo, P. A., Mignani, R. P. & Bignami, G. F., 1999, A&A, 347, 494

Hulleman, F., van Kerkwijk, M. H., Verbunt, F. W. M., Kulkarni, S. R., 2000,A&A, 358, 606

Halpern, J-P & Tytler, D., 1988, ApJ, 330, 201

Marshall, F. E., Gotthelf, E. V., Zhang, W., Middleditch, J. & Wang, Q. D., 1998, ApJ, 499, L179

Martin, C. Halpern, J. P. & Schiminovich, D, 1998, ApJ, 494, 211

McLaughlin M. A. & Cordes, J. M., 2000, ApJ, 538, 818

Middleditch, J. & Pennypacker, C., 1985, Nature, 313, 659

Mignani, R. P., Caraveo, P. A., & Bignami, G. F., 1998, A&A, 332, L37

Mignani, R. P., Pulone, L., Marconi, G. Iannicola, G. & Caraveo, P. A., 2000, A&A, 355, 603

Nasuti, F. P., Mignani, R., Caraveo, P. A. & Bignami, G. F., 1997, A&A, 323, 839

Nice, D. J., Taylor, J. H. & Fruchter, A. S., 1993, ApJ, 402, L49

Pavlov G. G., Welty, A. D. & Cordova, F. A., 1997, ApJ, 489, L75

Pacini, F., 1971, ApJ, 163,17

Pacini, F. & Salvati, M., 1983, ApJ, 274, 369

Pacini, F. & Salvati, M., 1987, ApJ, 321, 445

Perryman, M. A. C., Favata, F., Peacock, A., Rando, N. & Taylor, B. G., 1999, A&A, 346, 30

Romani, R. W., & Yadigaroglu, I.-A., 1995, ApJ, 438, 314

Romani, R. W., Miller, A. J., Cabera, B. & Figueroa-Feliciano, E., 1999, ApJ, 521, L151

Shearer, A., Redfern, R. M., Gorman, G., Butler, Golden, A., R., O'Kane, P., Golden, A., Beskin, G. M., Neizvestny, S. I., Neustroev, V. V., Plokhotnichenko, V. L. & Cullum, M., ApJ, 1997, 487, L181

Shearer, A., Harfst, S., Redfern, R. M., Butler, R., O'Kane, P., Beskin, G. M., Neizvestny, S. I., Neustroev, V. V., Plokhotnichenko, V. L. & Cullum, M., 1998, A&A, 335, L21

Smith, F. G., Jones, D. H. P., Dick, J. S. P. & Pike, C. D., 1988, MNRAS, 233, 305

Thompson, D. J. et al, 1996, ApJ, 465, 385

Thompson, D. J. et al, 1999, ApJ, 516, 297

, Vasisht, G. & Gotthelf, E. V., 1997, ApJ, 486, L129

Wallace, P. T. et al. 1977, Nature, 266, 692

Wei, D. M., Song, L. M. & Lu, T., 1997,å, 323, 98

This manuscript was prepared with the AAS LaTeX macros v5.0.

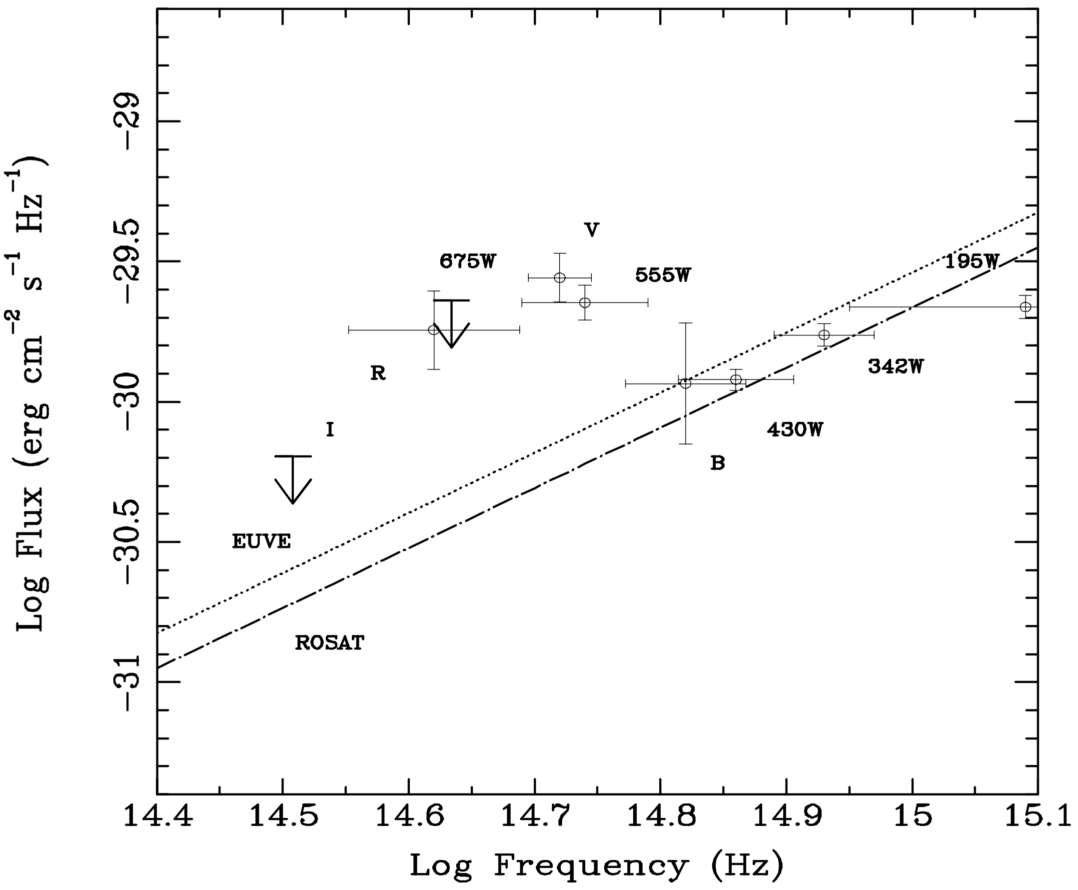

Fig. 1.— Photometry of Geminga. The integrated photometry and the thermal fit to the ROSAT X-Ray and EUVE data are both shown.

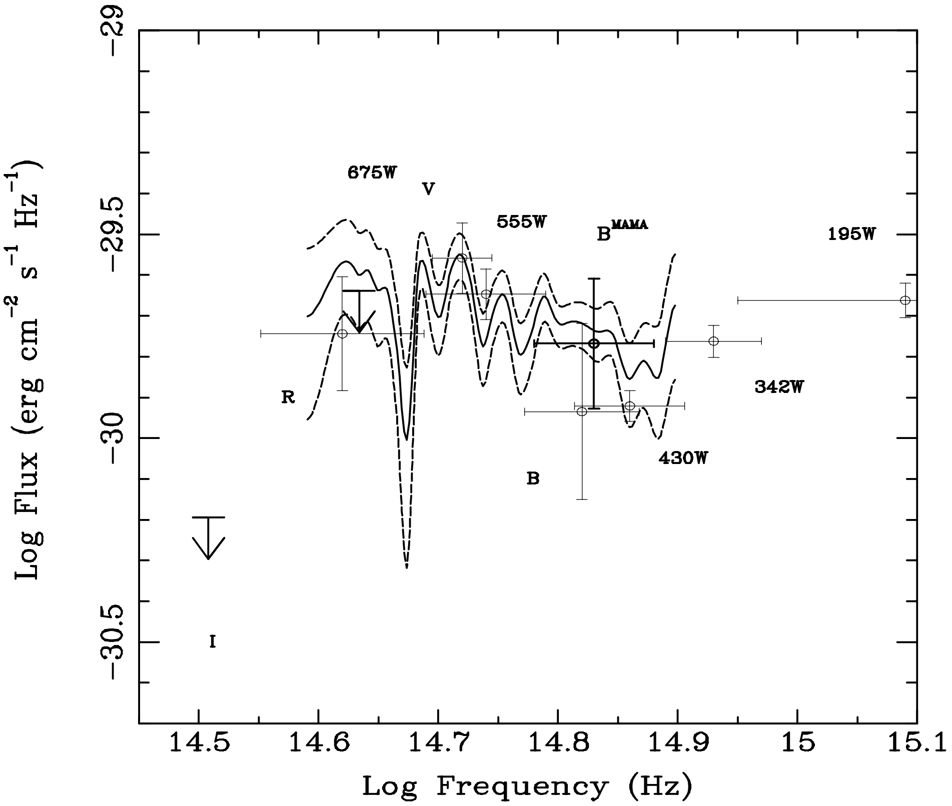

Fig. 2.— Spectra and Photometry of Geminga. The spectrum taken from (18) (solid line) and 1 σ error limits (dotted line) are shown. Note the agreement between it and the integrated photometry from Figure 1. B^{MAMA} is the pulsed flux from (33) and other points are from (21) and (3).

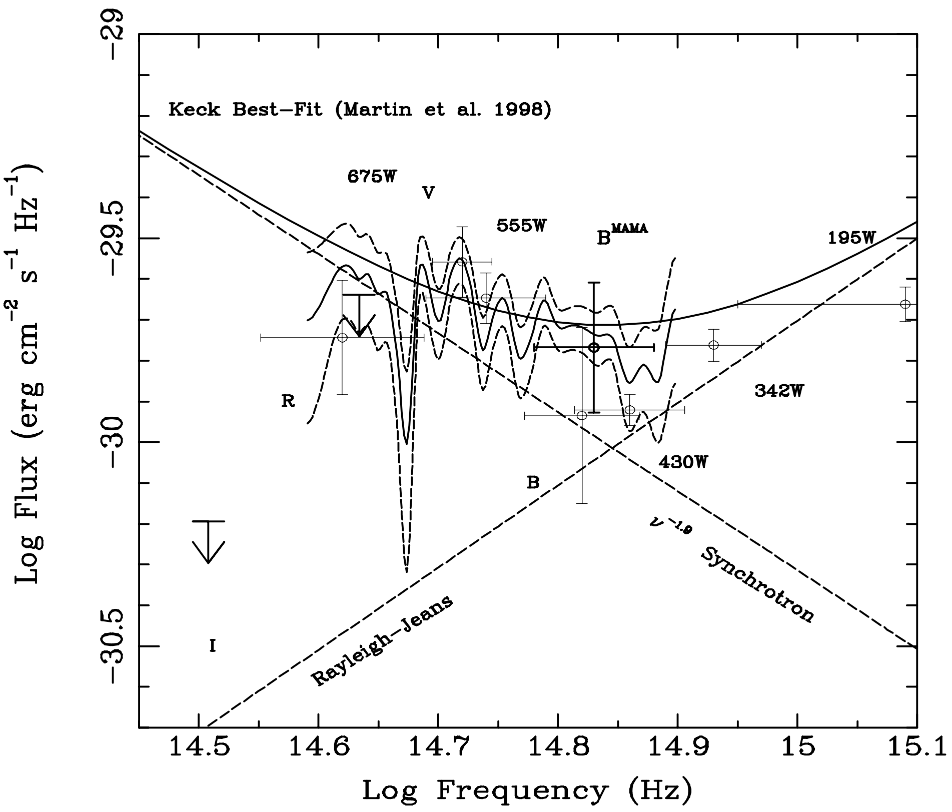

Fig. 3.— Derived thermal and non-thermal components for Geminga. Also plotted are the broad-band points points from figures 1 and 2.

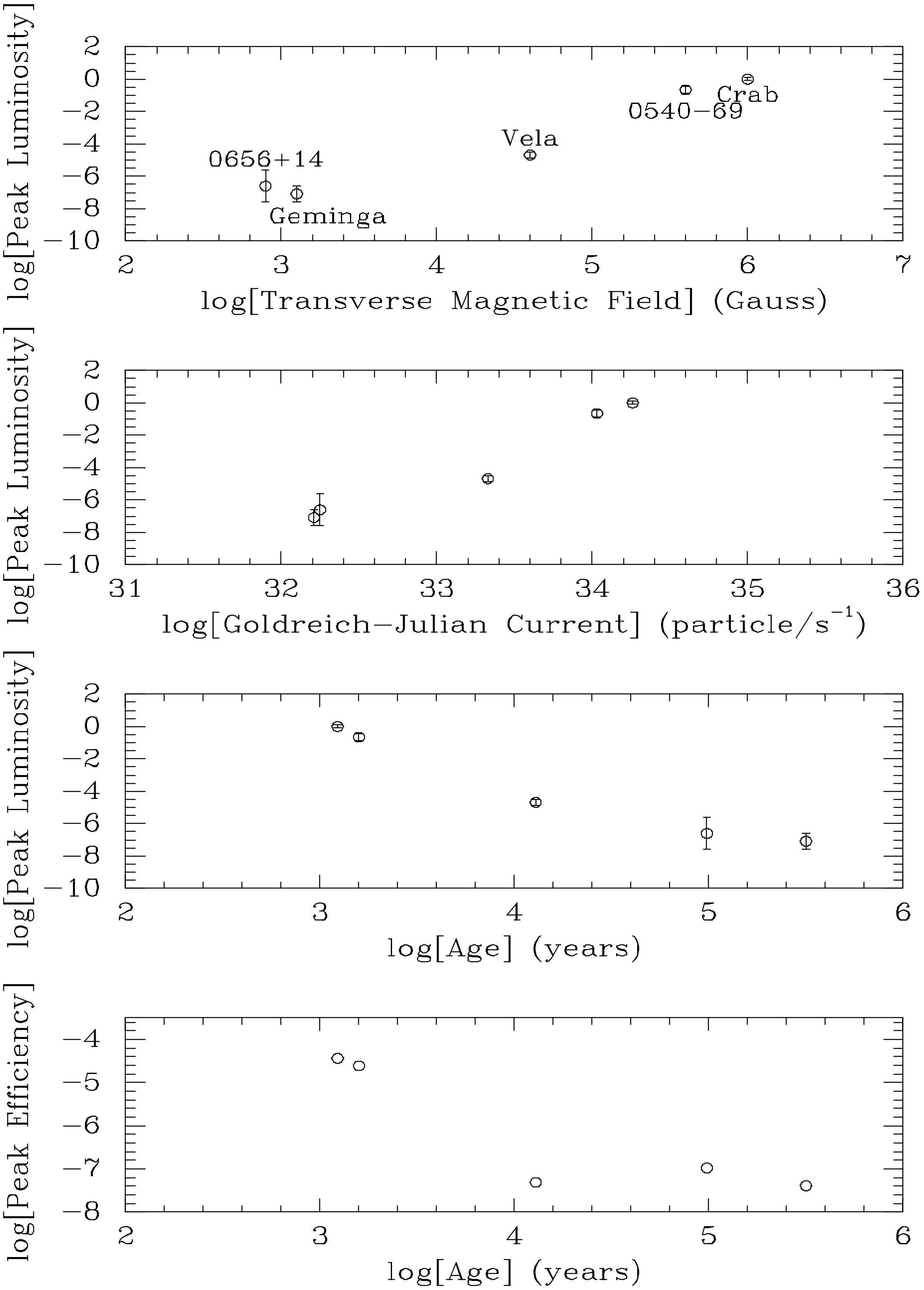

Fig. 4.— Peak optical luminosity vs light cylinder field, Goldreich & Julian current and canonical age. Also shown is the efficiency of the peak emission against age. The peak luminosity has been normalised to the Crab pulsar. The error bars represent both statistical errors from the pulse shape and uncertainty in the pulsar distance.

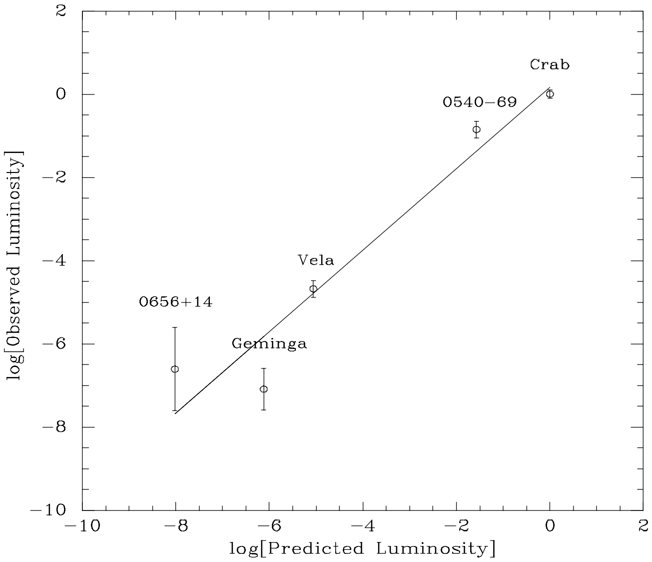

Fig. 5.— Predicted peak optical luminosity from equation 2 versus observed peak emission. Also shown is the weighted fit described in the text. The weighting was based upon the observational uncertainities in flux and distance.

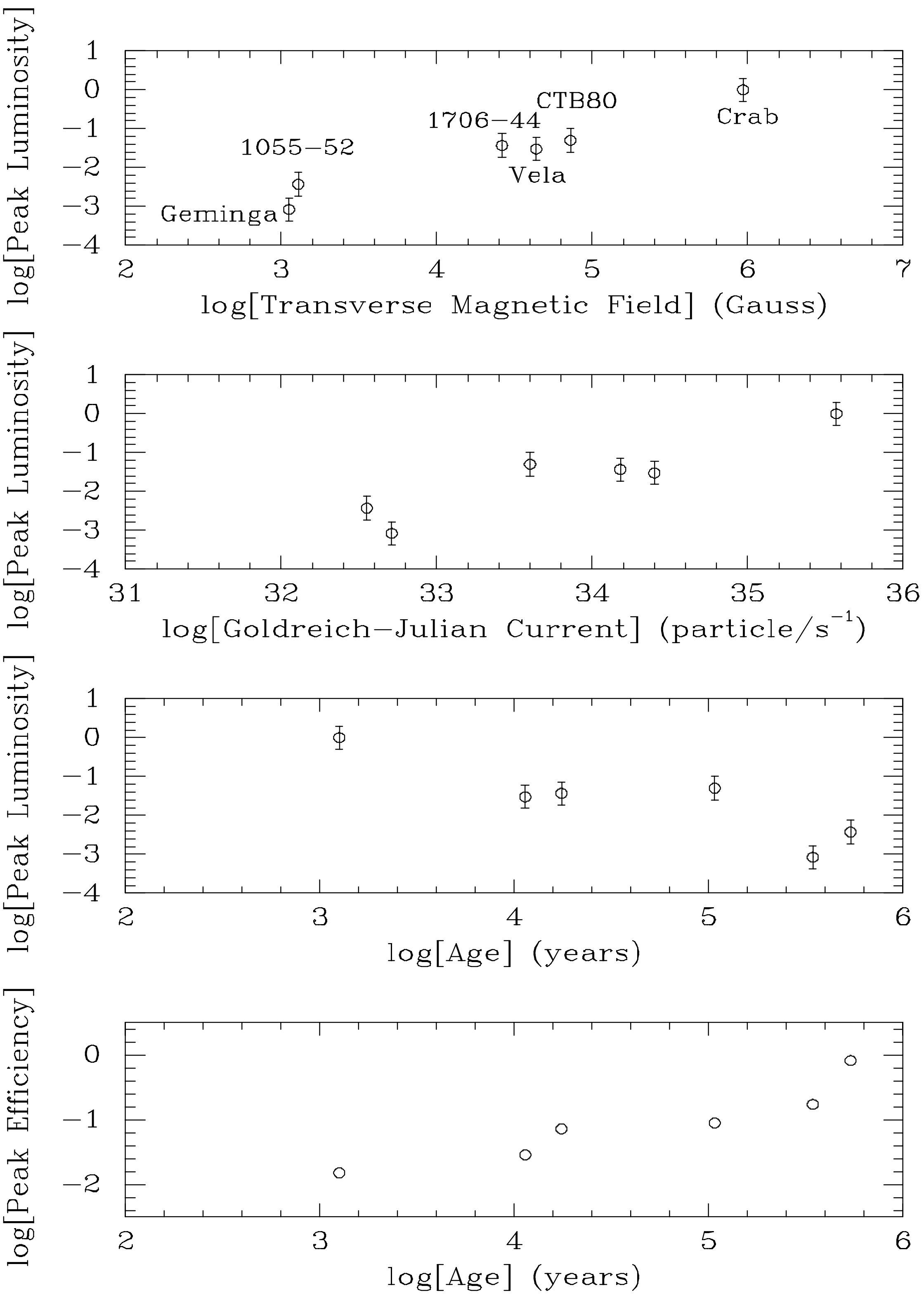

Fig. 6.— Peak γ-ray luminosity vs light cylinder field, Goldreich & Julian current and canonical age. Also shown is the efficiency of the peak emission against age. The peak luminosity has been normalised to the Crab pulsar. The γ-ray peak luminosity has been inferred from (7), (35) and (36).

Table 1: Main characteristics of Optical Pulsars: B_S & B_{LC}, the canonical surface and transverse magnetic field at the light cylinder respectively; Int and Peak refer to the optical luminosity, integrated and peak, at the indicated distance in the B band.

Name	D	P	$\dot{P}$	Log Age	B_S	B_{LC}	Int	Peak	Spec. Index	Cutoff
	(kpc)	(ms)	10^{-14} s/s	Years	log(G)	log (G)	μCrab	μCrab	at 4500 Å	Å
Crab	2	33	42	3.09	12.6	6.1	10^6	10^6	-0.11	15000(?)
Vela	0.5	89	11	4.11	12.5	4.8	27	21	0.2	6500(?)
PSR0545-69	49	50	40	3.20	12.7	5.7	1.1 10^6	1.4 10^5	0.2	>7000
PSR0656+14	0.25(?)	385	1.2	5.50	12.7	3.0	1.8	0.3	1.3	>8000
PSR0633+17	0.16	237	1.2	4.99	12.2	3.2	0.3	0.1	1.9	>8000

Table 2: Main characteristics of γ-ray Pulsars: B$_S$ & B$_{LC}$ the canonical surface and transverse magnetic field at the light cylinder respectively; γ Int and Peak refer to the integrated and peak γ-ray luminosity at the indicated distance for E > 100 MeV.

Name	D	P	$\dot{P}$	B_S	B_{LC}	Int Lumin.	Peak Lumin.	Spectral Index
	(kpc)	(ms)	10^{-14} s/s	log(G)	log (G)	Crab=1	Crab=1	
Crab	2	33	42.1	12.58	5.97	1	1	2.15
Vela	0.5	89	12.5	12.53	4.64	0.0480	0.0299	1.70
PSR1055-52	0.5-1.5	197	0.6	12.03	3.11	0.0124	0.0037	1.18
PSR1706-44	2.4	102	9.3	12.49	4.42	0.1380	0.0368	1.72
PSR0633+17	0.16	237	1.1	12.21	3.05	0.0019	0.0008	1.50
PSR1951+32	2.5	40	0.6	11.69	4.86	0.0500	0.0187	1.74

Table 3: Predicted Luminosity of X and γ-ray emitting pulsars. The duty cycle has been estimated from γ-ray observations. Also included are the nearby millisecond pulsar PSR J2322+2057 ((24)) and the anomolous X-ray pulsar 1E1841-045 ((Vasisht & Gotthelf)).

Name	D	P	$\dot{P}$	B_S	B_{LC}	Duty	Pred. Lumin.
	(kpc)	(ms)	10^{-14} s/s	log(G)	log (G)	Cycle	μCrab
PSR1055-52	1.5	197	0.6	12.03	3.11	0.2	0.01
PSR1706-44	1.8	102	9.3	12.49	4.42	0.14	35
PSR1951+32	2.5	40	0.6	11.69	4.86	0.08	670
PSR1821-24(M28)	5.1	3	1.1^{-4}	9.3	5.8	0.1	0.3-1 10^6
PSRJ2322+2057	0.78	4.8	7.0^{-7}	8.3	4.2	0.3(?)	8
1E1841-045	7	11770	4700	≈ 15	-2	0.5?	$<< 10^{-10}$